Environmental Science Nano

ROYAL SOCIETY OF CHEMISTRY

PAPER

View Article Online
View Journal | View Issue

Cite this: *Environ. Sci.: Nano*, 2024, 11, 889

Particles in a box: novel design and evaluation of an adaptable engineering control enclosure for a common split tube furnace to eliminate occupational exposure to refractory ceramic insulation fibers†

Nina Z. Janković, [abc] Wei Lee Leong,[d] Andrew I. Ryan,[e] Omar N. Tantawi,[b] Brian S. Smith[d] and Desiree L. Plata [*bc]

Split tube furnaces, which rely on insulation commonly made of refractory ceramic fiber (RCF) material, are routinely used in nanotechnology laboratories to generate carbon-based nanomaterials and other manmade materials through chemical vapor deposition (CVD) processes. RCF aerosols can pose a use-phase inhalation risk to operators. We quantified the inhalation exposure risk and designed, built, and tested the impact of a benchtop ventilated enclosure for a common split tube furnace. Direct real-time measurements revealed that traditional use of the furnace could result in peak RCF total and respirable fraction particle mean concentrations of 25 ± 10 mg m^{-3} and 11 ± 4 mg m^{-3}, respectively (n = 50). Employment of the ventilated enclosure reduces instantaneous exposure to total RCF dust and the respirable fraction to approximately baseline values: 0.006 mg m^{-3} ± 0.003 mg m^{-3}, and 0.003 mg m^{-3} ± 0.002 mg m^{-3}, respectively (n = 30). The peak concentration of suspended particulate matter is highly variable over uniform release triggers, ranging from 5–50 mg m^{-3} for PM_{TOTAL} and 2–18 mg m^{-3} for $PM_{RESPIRABLE}$. Electron microscopic examinations of collected airborne materials were conducted to count the airborne number concentrations of RCFs greater than 5 μm in length, less than 3 μm in width, and that met a 5 : 1 length : width aspect ratio minimum, which are of toxicological concern. Concentrations of those RCFs were similarly reduced when the enclosure was in place. Technical drawings and specifications of the split tube furnace enclosure design are available for ready recreation and implementation, in light industry or laboratory settings, thereby providing low-cost modification to protect the health of workers and researchers.

Received 18th January 2023,
Accepted 17th January 2024

DOI: 10.1039/d3en00041a

rsc.li/es-nano

Environmental significance

Split tube furnaces are among the most common laboratory devices used to synthesize carbon-based nanomaterials by chemical vapor deposition. This work illustrates that certain use scenarios can lead to unnecessary exposure to furnace insulation materials that may lead to health concerns. We present a low-cost mitigation technology to protect occupational health.

1. Introduction

Catalytic chemical vapor deposition (CVD) is used to produce a wide variety of carbonaceous materials, including carbon nanotubes (CNTs),[1] graphene,[2] boron nitride nanotubes (BNNTs),[3] and other advanced and hierarchical materials.[4–8] A common feature of CVD is high-temperature processing (*e.g.*, 400–1200 °C) that requires the presence of insulative materials to reduce thermal losses and improve temperature control and stability. A favored insulative material with high thermal stability are refractory ceramic fibers (RCFs) often used with clamshell furnaces. Due to their size and the cost of ventilation systems (*e.g.*, hoods or glovebox enclosures), these furnaces are frequently used in open workspaces. This creates a potential

[a] *Department of Chemical and Environmental Engineering, Yale University, New Haven, CT, 06511, USA*
[b] *Department of Civil and Environmental Engineering, Massachusetts Institute of Technology, Cambridge, MA 02142, USA. E-mail: dplata@mit.edu; Tel: +1 617 258 8596*
[c] *Center for Green Chemistry and Green Engineering, Yale University, 225 Prospect Street, New Haven, CT, 06520, USA*
[d] *Environmental Health and Safety, Massachusetts Institute of Technology, Cambridge, MA 02142, USA*
[e] *MIT Central Machine Shop, Massachusetts Institute of Technology, Cambridge, MA 02142, USA*

† Electronic supplementary information (ESI) available. See DOI: https://doi.org/10.1039/d3en00041a

exposure hazard to RCFs, especially when the clamshell is agitated; the health impacts of this have yet to be evaluated. Such exposure would have important consequences for the workforce of carbon nanomaterial and advance composite fabrication, and this becomes increasingly important as the industries continue to grow.

RCFs are amorphous fibers that belong to the class of synthetic vitreous fibers (SVFs), also known as manmade mineral fibers (MMMF). RCFs are produced by melting calcined kaolinite ($Al_2Si_2O_5[OH]_4$), or a mixture of alumina (Al_2O_3) and silica (SiO_2) in approximately equal portions.[9] Other oxides, such as ZrO_2, TiO_2, B_2O_3, and Cr_2O_3 are occasionally added in smaller amounts to modify fiber properties, such as durability and heat resistance.[10,11] Subsequently, bulk fibers are formed by either *blowing* or *spinning* the molten material, commonly yielding up to 80% w/w fibers (product), and 20–50% w/w nonfibrous particulate (byproduct; *i.e.*, "shot").[9,11,12] The resultant chemical compositions vary with approximately 50% w/w silica, 35–50% w/w alumina, and less than 1–15% w/w other oxides, most notably zirconia.[9] At service temperatures in excess of approximately 980 °C over extended periods of time, RCFs partially convert to the silica polymorph cristobalite through devitrification.[11,13,14] The devitrification rate is dependent on temperature and time, and the resultant material is commonly referred to as "*after-service fiber*".[9,15]

Fibrous particles are physical toxicants, whose toxicity uniquely depends on their geometry, where fibers are characterized by large aspect ratios (length-to-diameter ratios).[16] The pathogenicity of inhaled fibers is controlled by the coordinated effects of the dose, dimension, and durability of fibrous particles (known as the "3D paradigm" of fiber toxicity).[16–18] These 3Ds are interrelated; for example, the length of inhalable fibers deposited in the lung is a primary determinant of fiber residence time.[16,18] Biopersistence is a measure of fiber residence time in the lung, and it incorporates breakage, dissolution, and mechanical clearance phenomenon.[16,17] Natural mineral fibers, such as asbestos minerals, are crystalline and fracture longitudinally along cleavage planes, under mechanical stress, resulting in acicular (*i.e.*, needle-shaped) fragments.[18] Consequently, fragmentation of asbestos fibers produces a larger number of asbestos fibers with decreased diameters, while retaining their lengths. Conversely, RCFs are amorphous fibers that fracture transversely, producing shorter fibers with the same diameters, which may be cleared by macrophages.[18,19] This capacity to fracture transversely after deposition in the lower respiratory tract translates to a lower biopersistence for RCF (88 days in rodents) than for asbestos fibers (1000 days for amosite and crocidolite);[16,20] in spite of the difference, RCF are not toxicologically benign.

Several animal studies of chronic nose-inhalation showed that rodents exposed to high levels of RCFs developed fibrosis and tumors (lung cancer or mesothelioma), indicating RCFs were persistent long enough to cause lung pathologies.[10,11,20–22] The International Agency for Research on Cancer (IARC), classified RCF as possibly carcinogenic to humans (Group 2B) based on sufficient evidence for carcinogenicity in experimental animals, but inadequate evidence in humans.[12] Similarly, "[o]n the basis of a weight-of-evidence carcinogenic risk assessment, the EPA[23] [also] classified RCFs as a Group B2 carcinogen (probable human carcinogen based on sufficient animal data)."[9] As such, prudent guidelines for limiting occupational RCF exposure have been in place for over three decades.[10,23,24] National Institute for Occupational Safety and Health (NIOSH) established a recommended exposure limit (REL) of 0.5 f cm^{-3} as a time-weighted average (TWA) for up to a 10 h work shift in a 40 h workweek, where "reasonable efforts" should be made to reduce exposure below 0.2 f cm^{-3}.[9] In spite of this recommendation, no legally enforceable, Occupational Safety and Health Administration (OSHA) permissible exposure limit (PEL) exists for RCFs, apart from the California Division of Occupational Safety and Health (Cal/OSHA) PEL of 0.2 f cm^{-3} in California.[25] However, RCF exposures have successfully been monitored and controlled through a voluntary product stewardship program, an industry-wide program developed by RCF manufacturers (overseen by OSHA) to identify and control risks associated with manufacture and use of RCF-containing products.[10] While the stewardship program successfully decreased average fiber exposure concentrations for both manufacturers and customers,[10,26] the many RCF-lined furnaces are found in research laboratory settings are not part of the program. Considering just our own university as a representative sample, we found the use of furnaces to be prevalent, with 218 registered furnaces spread over 1021 principal investigators (including faculty without labs), on Massachusetts Institute of Technology's (MIT) campus alone.

In campus settings, Environmental Health and Safety (EHS) departments are not required or compelled to monitor the release of RCFs from these commonly used furnaces, because it is not obvious that there is an imminent occupational hazard associated with use of clamshell furnaces. (Here we note that many campus EHS units do recommend enclosure, ventilation, exhaust for furnaces that use or generate hazardous chemicals or vapors). However, certain furnace configurations have exposed insulation or have operation routine that requires access to insulated compartments, and this motion can disturb the insulation, incidentally releasing fibers into the air. In particular, benchtops below split-tube furnaces often have a thin coating of white dust, which could contain RCFs and alludes to the potential for user inhalation exposure.

To determine the possible dust and RCF exposures during laboratory-scale nanomaterial synthesis, we used a representative model furnace to investigate the possible peak dust and average RCF concentrations in the breathing zone during furnace use. We simulated use with agitation events and deployed both instantaneous and filter-based measurement techniques to gauge episodic and integrated exposures, as well as to characterize released materials. Finding some undesirable exposure scenarios, we present

designs for low-cost enclosures with dynamic motion accommodation to mitigate occupational risk to researchers associated with CVD nanomaterial production in split-tube clamshell furnaces. Importantly, this work provides some of the first measures of RCF exposure during the routine utilization of tube furnaces and provides a route for the safe utilization of these critical tools for discovery and advanced manufacturing.

2. Methods

2.1. Uncovered split-tube furnace and enclosure design

The subject of this study focuses on split-tube furnaces and a strategy to reduce exposure to particles generated by their use in the form of an enclosure. The former is commercially available and the later was custom built.

Two Lindberg/Blue M Mini-Mite furnaces (part number TF55030A-1) were used for aerosol and bulk RCF sampling. The furnace's exterior and insulation dimensions were $41L \times 28W \times 38H$ centimeters and $36L \times 16W \times 20H$ centimeters, respectively. The furnace can accommodate a 2.54 cm process tube diameter and has an internal heated zone of 30.5 cm in length. The age of the furnaces was approximately ten years.

A custom-built box enclosure (Fig. 1) was designed and constructed from clear acrylic and aluminum. The front, back, left, and right sides of the enclosure were made from clear acrylic for transparency. Note that polycarbonate is an alternative material that is less susceptible to melting or burning than acrylic, and that some fire codes place restrictions on the use of acrylic panels. The bottom of the enclosure was made using an aluminum plate connected to a block of plywood for mechanical stability. An aluminum plate was used for the top of the enclosure to ensure resistance to high-heat events associated with an open clamshell furnace. The benchtop enclosure was connected to local exhaust ventilation (*i.e.*, a snorkel).

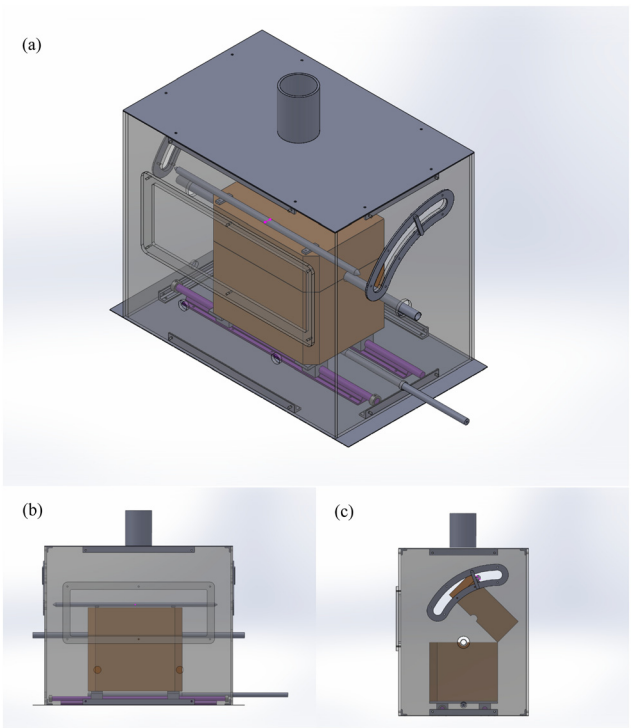

Fig. 1 Schematic of furnace inside ventilated enclosure. (a) 3-D view; (b) front view; (c) side view. Note the enclosure can accommodate two lengths of the Lindberg/blue M mini-mite furnace.

Two features provide dynamic motion of the furnace within the enclosure while it is sealed, slide rails and lid lifting handles. The slide rails allow for rolling of the furnace along the quartz tube (*e.g.*, to control the insertion of a substrate into the heated zone). The enclosure length can easily be modified to accommodate a traditional stationary furnace setup. Furnace lid lifting handles were fashioned from an aluminum rod and attached to the top of the furnace. These handles protrude from the left and right sides of the enclosure and are guided by a curved opening which follows the arched trajectory of lifting the furnace lid. Since vertical alignment of the furnace tube is sometimes desired or necessary with both the feed system at the tube inlet and the collection or further processing system at the tube outlet (each of which might be constrained in their vertical alignment due to weight, stability, or other limitations), the underside of the split tube furnace can be equipped with rugged, adjustable laboratory jacks. In such cases, the inlet and outlet openings of the enclosure could also be fabricated as vertical slots to readily allow vertical adjustments of the tube height.

An opening with a detachable cover was added to the front of the enclosure to provide full access to the inside of the box, which is intended for occasional use. This opening was sealed with a foam gasket and screws. Two 1.25 inch openings located at the front of the enclosure serve as inlets for air and are covered with MERV13 and high efficiency particulate air (HEPA) filters (to prevent particle discharge into the room in the case of air flow disturbance). All other openings (*i.e.*, furnace lid lifting handles, furnace rolling rod, quartz tube, furnace cable) were sealed with rubber sheets to control and limit the air flow to the designated air flow openings. The effluent from the quartz tube reactor is also directed to the enclosure for discharge. (Technical drawings and CAD files of the design are available by contacting the author).

In designing the enclosure to mitigate exposure to releases of RCF insulation material and facilitate furnace operation as described above, it is prudent Industrial Hygiene and Occupational EHS (IH/OEHS) practice[27] to ensure that the proposed enclosure design would not introduce or increase risks from other hazards. Other hazards associated with split tube furnace operations include (but are not necessarily limited to) pinch or crush injuries during positioning or manipulation of the furnace body and clamshell; electrical shock; thermal burns; cuts, puncture wounds, or eye injuries from contact with potentially broken or damaged ceramic tube materials; inhalation or dermal exposure to releases of RCF insulation

material during furnace setup, operation, maintenance, or decommissioning; and inhalation or dermal exposure to fugitive airborne releases of process materials from within the tube furnace during pre-operational, operational, and post-operational activities. Risks of exposure to these other hazards are not increased by the selected design.

2.2. Air sampling and agitation procedure

RCF aerosols are generated when exposed furnace insulation is physically disturbed, and the most aggressive daily operational disturbance in split tube furnaces occurs upon opening and closing of the furnace shell. To sample RCF aerosols, repeated cycles of opening and closing the furnace were performed (termed "agitation" events). Samples were taken close to the center of the tube furnace shell opening (Fig. S1†) while systematically agitating the RCF insulation. A single agitation event was defined as opening and closing the furnace ten times in succession. Samples were collected from two Lindberg/Blue M Mini-Mite furnaces (part number TF55030A-1) at room temperature, (1) without the enclosure and (2) with the enclosure. Baseline or blank room dust levels are measured without performing any agitations to the furnace.

2.3. Real-time measurements with DustTrak DRX

TSI DustTrak DRX (model number 8533) Aerosol Monitor was used to sample the air for real-time particle measurements. For samples collected outside of the enclosure, we sampled directly into the inlet of the DustTrak by positioning the instrument directly in front of the furnace opening at center. For sampling inside the enclosure, we utilized plastic tubing to access the space directly in front of the furnace at the furnace opening (Fig. S1†). Numerous agitation events were executed at three sampling positions (Fig. S1†), (A) without the enclosure (n = 50), (B) with the enclosure (n = 30), and (C) inside of the enclosure (n = 40). After each agitation, allowed time to for the aerosol concentration to return to the prior baseline.

2.4. *In situ* particle measurements with DustTrak DRX

The DustTrak DRX Aerosol Monitor used for real-time mass and size fraction particle measurements recorded measurements in 5 s intervals. HEPA-filtered air was used to zero the instrument, and the instrument was calibrated to ISO 12103-1 A1 ultrafine test dust. DustTrak assumes spherical particles to determine the mass concentration across the particle size bins. While most of the insulation aerosols are fibrous, nevertheless, we found excellent agreement with the calibration ISO 12103-1 A1 dust and the DustTrak readings by testing the size calibration factor as described in the manual.

The mass concentration was reported in mg m^{-3} for PM2.5 using a laser light-scattering photometer. The photometric signal combined with single particle optical sizing allows for the following size segregated mass distributions to be calculated: PM1, PM2.5, respirable (PM4), PM10, and total (greater than PM10).[28,29] The DustTrak DRX monitor has a mass concentration range of 0.001–150 mg m^{-3} and a particle size range of approximately 0.1–15 μm.[30]

2.5. Air sampling on filters for TEM analysis

In order to visualize collected particles, a NIOSH 7402 method (Asbestos by transmission electron microscopy (TEM)) adjusted for RCFs analysis was used.[31–33] Air samples were collected on 0.45 um mixed cellulose ester (MCE) membrane filters at a flow rate of 10 L min^{-1}, over 10 agitation events, at three sampling positions (Fig. S1†). Assembled filter cassettes were maintained in a vertical position and undisturbed while sampling. Blank samples were collected by treating assembled cassettes alongside samples but without pulling air through them. Two field blanks (stored in a clean area while sampling with the top covers removed) and one media blank (never opened cassette assembly which travels with the samples) were collected.

2.6. Bulk material sampling

In order to determine the nascent composition of the insulative material in the furnace, exposed insulation was collected from inside a Lindberg/blue M mini-mite furnace (part number TF55030A-1). Loose and scrapped particles were collected from the exposed surface of the furnace (*i.e.*, inside the clam-shell opening) with a stainless-steel spatula and transferred into a small glass vial until further analysis by TEM. To collect a sufficient mass of particles, the insulation was lightly scrapped with the metal spatula used for collection.

2.7. RCF analysis by TEM

Analysis was done by contract lab Bureau Veritas Inc. Industrial Hygiene Laboratory in Kennesaw, Georgia.[34] Briefly, MCE membrane filters were placed on a glass slide and a solution of dimethyl formamide/acetic acid was used to clear the filters (making them transparent). Next, the samples are partially ashed in a plasma asher, and carbon coated in a vacuum evaporator. Segments of the filters were placed on 200-mesh copper TEM grids in a wick-type solutional washer containing 100% acetone. Two grids were placed consecutively in the TEM for examination. Grid openings were examined by TEM-Phillips CM 12 and CM 10 with integrated X-ray fluorescence (IXRF) energy dispersive X-ray spectroscopy (EDS) system tungsten filament at 15 000× magnification. A minimum of 40 grid openings or 100 fibers were counted across two grids, selecting an approximately equal number of grid openings from each of the two grids. Grid openings were selected randomly across each grid for fiber counting. Fibers at least 2.5 μm in length for which only one end of the fiber was visible, were counted as 0.5 fibers. Only RCFs over 5 μm in length, less than 3 μm in width, and that met a 5:1 length:width aspect ratio minimum were counted. RCFs which met these criteria were identified by morphology, and energy dispersive X-ray spectroscopy (EDS). EDS served to confirm fibers had the appropriate chemical composition to be classified as RCFs.[35]

2.8. Bulk material characterization

Analysis was done by contract lab Bureau Veritas Inc. Industrial Hygiene Laboratory in Kennesaw, Georgia. A scanning electron microscope (SEM) Tescan Vega with IXRF (EDS) system tungsten filament was used to image the bulk material. A mixture of approximately 100 mg of bulk material was suspended in 5 ml of acetone and ultrasonicated for three minutes. Next, the sample was spun down by centrifuge for three minutes and the supernatant was decanted to a level of 0.5 ml. A drop of the remaining suspension was placed on each of two carbon-coated grids and characterized by TEM with IXRF (EDS) as described above. Materials are identified by morphology, selected-area electron diffraction (SAED), and energy dispersive X-ray spectroscopy (EDS).

The mass of individual counted fibers was estimated from the volume and density. For the calculation of volume, the lengths and widths of the fibers were directly measured, and the fibers were assumed to be cylindrical, as the third dimension could not be directly measured. The mass of individual particles (including aggregates) was estimated for approximately 60 particles or aggregates.

3. Results and discussion

3.1. Morphological, chemical, and size properties of RCFs

To investigate the material properties of the insulation, *i.e.*, structure, morphology, and chemical composition, we characterized a bulk sample by SEM, TEM, and EDS. Bulk material characterization assumes the bulk sample is homogeneous, representative of airborne particle fractions, and preserved throughout sample processing. SEM and TEM images reveal the presence of fibrous and nonfibrous particles (Fig. 2). EDS confirms fibers are RCFs with the following representative chemical compositions 46 wt% Al_2O_3 and 54 wt% SiO_2 (approximately $1Al_2O_3{\cdot}2SiO_2$). Nonfibrous particulate matter was aluminosilicate and silica particles with the following representative chemistries, also determined by EDS: $Al_2O_3{\cdot}SiO_2$ particles are 27 wt% Al_2O_3 and 73 wt% SiO_2 (approximately $1Al_2O_3{\cdot}4.5SiO_2$), and SiO_2 particles are 100% SiO_2.

In RCF manufacturing, the particle-to-fiber ratios range from 20 : 80 to 50 : 50 percent by weight.[9] Typically, the product (fibers) yield is 50% by weight, and the rest is byproduct (nonfibrous particulate).[9,11] To estimate the particle to fiber ratios of our bulk material, we analyzed 56 particles, by TEM; the fibrous content is approximately 80% by weight. The presence of nonfibrous nanoparticle agglomerates (mostly SiO_2) falsely increases the cumulative estimated mass; the thickness of particles is assumed to be equal to the width, since thickness cannot be directly measured. All particles were analyzed by SAED; only aluminosilicate particles diffracted. We note that these composition estimates agree with the disclosed chemical composition from the furnace manufacturer, under the trade name Moldatherm, (*i.e.*, 79–99% aluminosilicate and 1–21% amorphous silica).[14]

Exposure limits are established based on specific fiber size criteria. For an airborne particle to be counted as a fiber it must meet the following criteria: greater than 5 μm long, less than 3 μm diameter, and with an aspect ratio greater than or equal to 5 : 1 (NIOSH B rules). To investigate the size distribution of fibers, we measured the lengths and widths of RCFs for portions of the bulk sample and airborne fibers collected on filters (Fig. 3). EDS confirmed fibers in the airborne sample are RCFs with a chemical composition of 47 wt% Al_2O_3 and 53 wt% SiO_2 (approximately $1Al_2O_3{\cdot}2SiO_2$). Nearly all RCF lengths cluster below 50 μm for all measured fibers; 78% of fibers for the bulk sample are between greater than 0.1 and less than or equal to 1 μm in width, while 80% of fiber widths for the airborne sample without enclosure are between greater than 0.5 and less than or equal to 1.5 μm in width (Fig. 3). Overall, the fiber size distribution is similar between the bulk and airborne samples, which supports the assumption that the bulk material is representative of the airborne sample (Fig. 3).

In order to determine exposure to RCF, we analyzed the airborne samples to determine RCF concentration. We sampled across 10 agitation events (approximately 15 min), following

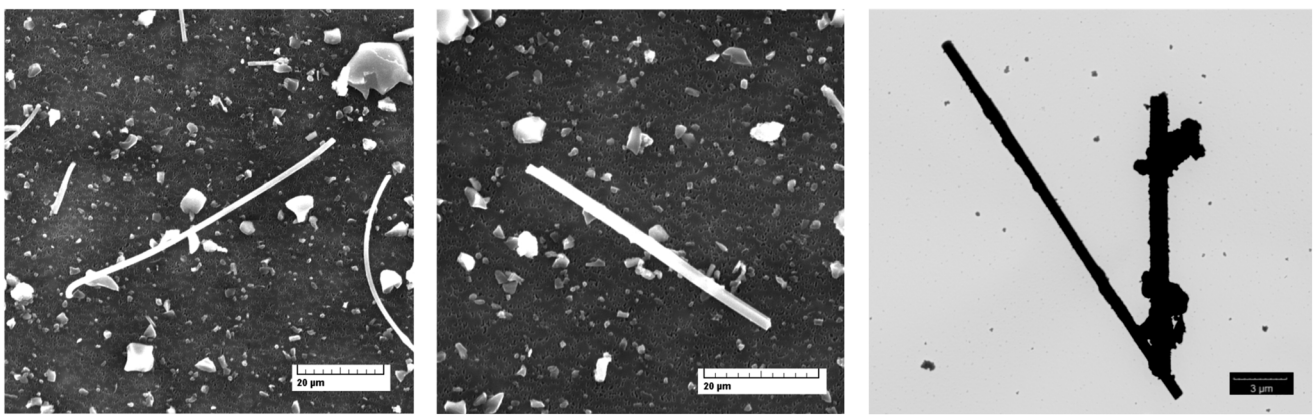

Fig. 2 Bulk material characterization by SEM and TEM. (a) and (b) are SEM images and (c) is a TEM images, centered around representative RCFs.

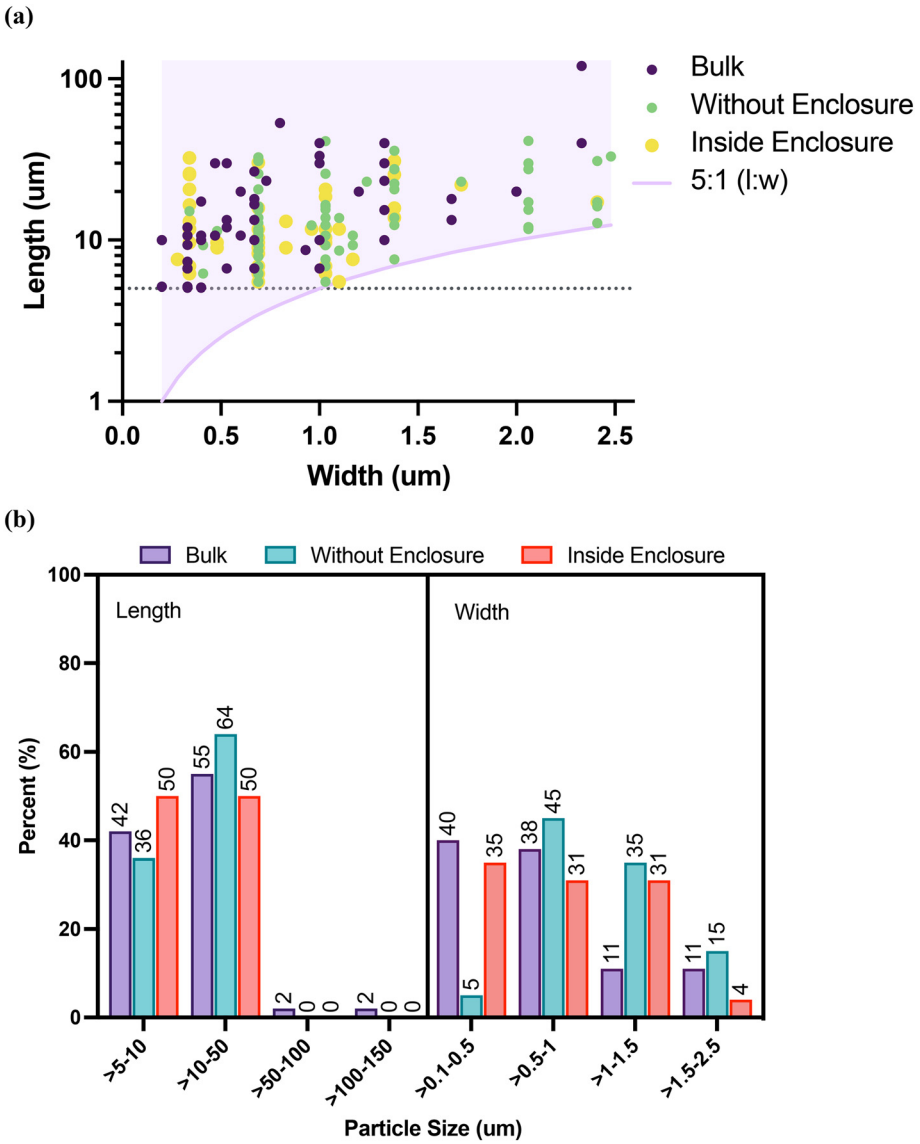

Fig. 3 Aerosol and bulk fiber size distribution. (a) RCFs greater than 5 μm in length, less than 3 μm in width, and with a greater than or equal to 5 : 1 length : width aspect ratio counted by TEM. Grey dotted line highlights the 5 μm length minimum. Purple curve represents 5 : 1 length : width aspect ratio for each measured particle width. (b) Fiber size distribution represented as a fraction across different size bins based on length or width of the fiber (1/2 fibers omitted, see ESI† for figure including 1/2 fibers).

NIOSH 7402 to collect and analyze the samples (expanded for RCF; using the "B" counting rules).[31–33] The average RCF concentration without the enclosure was 0.83 f cm^{-3}; this equates to an 8 h TWA of 0.0256 f cm^{-3} which approaches the ATSDR IMRC of 0.03 f cm^{-3}. This result suggests that if the set of agitations described were repeated 10 times throughout an 8 hour workday, the ACGIH TLV 0.2 f cm^{-3} exposure limit would be breached. No fibers were detected when the furnace enclosure was employed, demonstrating the effectiveness of the engineering control to contain RCFs.

3.2. Measurement of peak aerosol concentrations

Typical use of split tube furnaces does not generate aerosols continuously; rather, particles are released episodically upon disturbance of the RCF insulation. Real-time measurement of aerosol concentration allows for instantaneous monitoring and captures peak concentrations (Fig. S2†), whereas filter-based aerosol measurements fail to highlight these peak exposures because the particulate matter source is integrated through time. In order to determine the range of greatest potential exposures for a defined agitation, we analyzed peak concentrations (lasting ~5 s each) for 50 agitation events (Fig. 4) measured *via* DustTrak DRX. The peak total and peak respirable fraction particle concentrations were 25 ± 10 mg m^{-3}, and 11 ± 4 mg m^{-3}, respectively, exceeding the OSHA PEL (an enforceable, 8 h TWA) for total nuisance dust (15 mg m^{-3}) and the respirable fraction (5 mg m^{-3}) for particulates not otherwise regulated (PNOR) (Fig. 4).[36] Note that the California OSHA and American Conference of Governmental

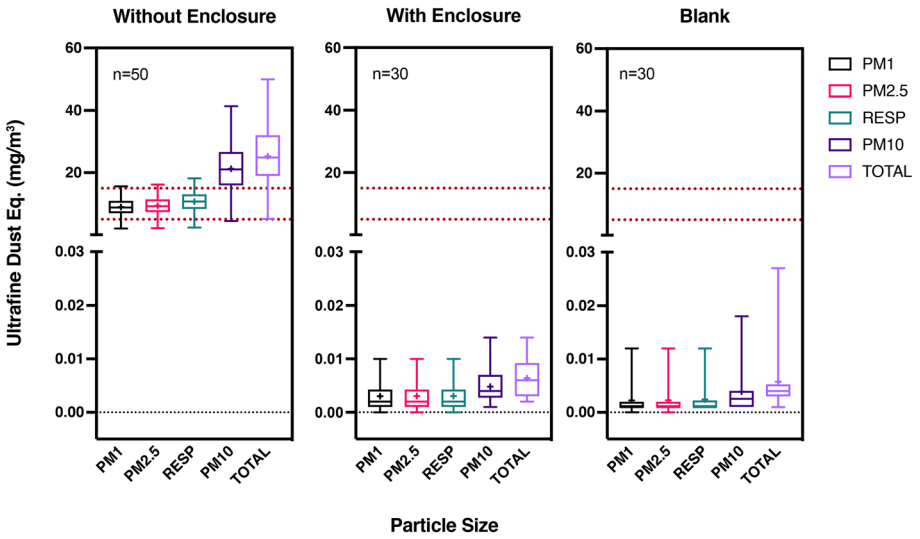

Fig. 4 RCF aerosol concentrations mitigated by ventilated enclosure. Particle concentration was measured with a DustTrak DRX in ISO 12103-1 A1 ultrafine test dust equivalents. Red dotted lines denote the OSHA PEL (8 hour TWA) for total nuisance dust (15 mg m^{-3}) and respirable fraction of particulates not otherwise regulated (PNOR) or "nuisance dust" (5 mg m^{-3}).[36] Box plots represent peak suspended particulate matter concentrations, where the crosses represent mean values, the line in the middle of the box represents the median, the hinges (top and bottom) of the box indicate the inner quartiles (25–75th percentile), and the whiskers represent the spread (minimum and maximum values) of all data. PM1, PM2.5, PM10, indicated the particle count for particulate matter (PM) less than 1, 2.5, and 10 micrometers in aerodynamic diameter assuming a spherical particle. RESP indicates the total respirable fraction (defined as less than 4 micrometers). TOTAL is the sum of all measured particulate matter.

Industrial Hygienists (ACGIH) recommend even lower exposure limits, where both recommend a 10 mg m^{-3} threshold for total particles and 5 or 3 mg m^{-3}, respectively, for respirable particles.[9,25,36] While peak concentrations and TWAs cannot be directly compared, our finding that these recommendation limits are greatly exceeded during agitation events indicates that it is *possible* to exceed the OSHA PELs for PNOR depending on the duty cycle and procedure (*i.e.*, the operator's practice and frequency of furnace use). Further, the disturbance actions resulted in a broad range of peak concentrations, ranging from 5–50 mg m^{-3} for total dust and 2–18 mg m^{-3} for the respirable fraction. Taken together, the resultant exposure from a single furnace can vary dramatically for each use, even for the same operator, and may exceed OSHA PELs for PNOR, depending on the frequency and intensity of operational disturbances.

Real-time measurements using DustTrak DRX are useful to estimate RCF exposure, but do not distinguish between fibrous and non-fibrous suspended particulate matter. The geometry of the particle has important implications for the toxicity. Thus, to estimate peak fiber concentrations, we converted the total peak mass concentration (Fig. 4) to estimated fiber concentrations using the median (0.02 ng f^{-1}) or the 97% confidence intervals (lower 0.01 ng f^{-1} or upper 0.03 ng f^{-1}) or the minimum (0.002 ng f^{-1}) or the maximum (0.4 ng f^{-1}) airborne fiber mass and a range of particle-to-fiber ratios. The particle-to-fiber ratios were chosen based on TEM measurements as discussed earlier (20 : 80 wt%) and shot content (20–50 wt%).[9,19] Mean airborne fiber mass was not considered because the standard deviation was larger than the mean. The mass of individual fibers was estimated from the volume and density. To determine volume, the lengths and widths of the fibers were measured *via* imaging and assumed to be cylindrical. The airborne fiber mass (ng f^{-1}) statistics were calculated from a subset of fibers, which all meet particular fiber size criteria (greater than 5 μm long, less than 3 μm in diameter with an aspect ratio greater than or equal to 5 : 1). Converting from mass to fiber concentration involves two key limiting assumptions: (1) the subset of fiber masses considered is a representative sample of fiber mass distribution, and (2) a sample size of 85 fibers is representative of the fiber distribution.

The sample of fibers considered does not have a normal distribution, which is evidenced by a standard deviation greater than the mean fiber mass. Therefore, we estimate the mass per fiber using the median fiber mass. Further, we bound the median by considering the upper and lower confidence intervals at 97%. Additionally, to show the range of values considered, we utilize the minimum and maximum mass per fiber.

We calculated that peak total fiber concentrations were on the order of 10^3 f/cm^3 based on median mass fiber and mean peak mass concertation (DustTrak). The lowest calculated peak fiber concentration was 30 ± 10 f cm^{-3} and ranged 6–60 f cm^{-3} (Table 2). Even the lowest values exceed the proposed excursion limit for RCFs in the range of 0.3–5 f cm^{-3}. The proposed excursion limit is discussed in greater detail below.

We only measured fibers that met the criteria defined under NIOSH 7402 and 7400 B rules,[31–33] therefore the fiber mass used was not representative of the true fiber mass distribution. Nevertheless, we find that even the lowest fiber concentrations surpass proposed short-term exposure limits proposed below. Further to partially resolve the constraints on the fiber mass, we use a wide range on fiber masses to calculate possible peak fiber concentrations (Table 2).

Table 1 RCF concentrations determined by modified NIOSH 7402. Field and media blanks are below the reporting limit of 2.3 f mm^{-2}; sensitivity is the limit of detection of the approach reported by Bureau Veritas North American[34]

	RCF concentration (f cm^{-3})	Sensitivity (structures per cm^3)	95% CI (low–high)	8 h TWA (f cm^{-3})
Without enclosure	0.83	0.0081	0.57–1.2	0.0256
With enclosure	<0.0079	0.0079	0–<0.035	<0.0002
Inside enclosure	0.40	0.0067	0.26–0.60	0.0112

In the absence of an OSHA PEL for RCFs, we can refer to the following 8 h TWA exposure limits NIOSH REL of 0.5 f cm^{-3}, American Conference of Governmental Industrial Hygienists (ACGIH) threshold limit values (TLV) of 0.2 f cm^{-3}, and agency for toxic substances disease registry (ATSDR) inhalation minimal risk concentration (IMRC) 0.03 f cm^{-3} exposure limits.[9] Note that the NIOSH REL was established as a TWA for up to a 10 h work shift in a 40 h workweek. Estimated peak fiber concentrations (Table 1) notably exceed the recommended TWA exposure limits. While the TWA exposure limits cannot be compared directly to peak values, exceeding time weighted limits for any amount of time, particularly for a highly variable fiber release process, suggests that it is possible to exceed the limit under some use scenarios or circumstances.

Further, in the absence of a ceiling, short-term exposure limits (STEL), or immediately dangerous to life or health (IDLH) limits for RCFs, we may consider the way in which asbestos is regulated. The 8 h TWA exposure limit OSHA PEL for asbestos is 0.1 f cm^{-3}, with an excursion limit of 1.0 f cm^{-3} averaged over any 30 minute sampling period.[37] The excursion limit for asbestos is an order of magnitude greater than the PEL, and we could employ this as a proxy to estimate the STEL for RCFs. Consequently, an estimate for a recommended excursion limit for RCFs may be in the range of 0.3–5 f cm^{-3} based on the recommended time-weighted exposure limits from various agencies listed above. Peak fiber concentration estimates are well above the upper limit of the approximate excursion limit (raised tenfold above the 8 h TWA).

3.3. Comparison of real-time measurements and NIOSH 7402

Direct measurement using the DustTrak allows for temporal resolution of particulate concentration, which is useful for tracking fluctuations present in episodic exposure. However, this measurement does not distinguish fibrous particles from nonfibrous particles. Furthermore, the fibrous fraction had a wide fiber size distribution, only a portion of which meet the NIOSH A or B rules for counting. The fibers that met the criteria had aspect ratios ranging from 5–97, which may not be accurately captured by the size bins of the DustTrak.

Conversely, the NIOSH method 7402 for sampling and analysis of fibrous material, provides an integrated sample from which the average fiber concentration is determined, which masks the peak concentrations found in episodic exposures. Concurrently, this method enables exact and explicit determination of fiber concentration for a subset of fibers with particular sizes defined by NIOSH A or B rules for counting fibers.

While sampling by NIOSH 7402 method, DustTrak was run in parallel, which permitted a direct comparison of the resultant average fiber concentration to the average mass concentration. We related peak mass concentrations to peak fiber concentrations through a conversion factor, mg f^{-1}. We found a peak total fiber concentration of 6 ± 2 f cm^{-3} (equivalent to PM_{TOTAL} 25 ± 10 mg m^{-3}), and a range of 1.2–12 f cm^{-3} (equivalent to PM_{TOTAL} 5–50 mg m^{-3}).

To protect the furnace operators from potential excursions in (1) fiber concentrations above the approximate excursion limits for short term exposures, (2) the time weighted exposure limits for fibers, and (3) the OSHA PEL for PNOR for both total dust and respirable dust fractions, we built a custom ventilated enclosure (Fig. 1 and S1†).

3.4. An engineering control for RCFs: furnace enclosure efficacy

In order to determine the effectiveness of our bench-top furnace enclosure, we sampled the air while agitating the

Table 2 Estimated fiber concentration from DustTrak mass concentration. Conversions of mass to fiber concentration based on the particle to fiber ratio and median, lower and upper confidence intervals, minimum, and maximum mass per fiber values. Mass per fiber values based on fibers collected on filters in "without enclosure" scenario. Half fibers were excluded; n = 85 fibers; a 97% confidence interval (CI) was considered

PM_{total} (mg m^{-3})	Mass per fiber (ng f^{-1}) considered		Fibers total (f cm^{-3}) *Particle-to-fiber ratio 20 : 80 (wt%)*	Fibers total (f cm^{-3}) *Particle-to-fiber ratio 50 : 50 (wt%)*
25 ± 10 (mean ± st dev)	*Median*	0.02	1000 ± 400	700 ± 200
	97% CI (lower bound)	0.01	1000 ± 500	900 ± 300
	97% CI (lower bound)	0.03	700 ± 300	400 ± 200
	Min	0.002	10 000 ± 4000	6000 ± 2000
	Max	0.4	50 ± 20	30 ± 10
5–50 (range: min–max)	*Median*	0.02	200–2000	100–1000
	97% CI (lower bound)	0.01	300–3000	200–2000
	97% CI (lower bound)	0.03	100–1000	90–900
	Min	0.002	2000–20 000	1000–10 000
	Max	0.4	10–100	6–60

furnace insulation (1) without the enclosure, and (2) with the enclosure. We found a dramatic decrease in airborne particles when the furnace was inside of the enclosure (Fig. 4 and Table 1). The peak total and respirable fraction particle mass concentrations fell to 0.006 ± 0.003 mg m^{-3} and 0.003 ± 0.002 mg m^{-3} from 25 ± 10 mg m^{-3} and 11 ± 4 mg m^{-3}, respectively. The 8 h TWA fibers concentrations fell to less than 0.0002 f cm^{-3} from 0.0256 f cm^{-3}. The level of total dust is reduced to baseline levels when the furnace is operated inside of the enclosure. We note that total dust levels of the furnace with the enclosure are slightly above the blank values due to expected disturbances around the instrument while agitating the furnace inside of the enclosure. We did not measure any particles in the air space outside of the enclosure when operating the enclosed furnace (Fig. 4 and Table 1), but are confident that these particles were being generated inside the enclosure (Table 1 and Fig. S3†).

3.5. Enclosure cost

Our engineering control can accommodate custom reactor set-ups, which may be constrained by the dimensions of a standard chemical fume hood. The enclosure contains any dust generated, while retaining the function of a split-tube furnace (*e.g.*, ability to position substrate or catalyst, or open the furnace for rapid cooling). Contrary to a properly functioning fume hood, which requires the sash to be lowered, restricting access to the furnace. Further, the cost of our enclosure is lower than that of a fume hood, $782.82 per linear ft. *versus* $1200–2500 per linear ft., respectively.[38] The enclosure is designed to cover only the footprint of the furnace, rather than an entire reactor setup, thus the enclosure footprint is lower than that of a standard 6 foot fume hood, with a total cost of approximately $2000 (or $450 per square foot) (Table S1†). Precise pricing of a fume hood is challenging to obtain as various features dramatically affect the cost. For comparison, the total cost of a 6 foot fume hood averages around $8000 on the lower-end, and approximately $57 000 for high-end hoods.[38] Although, our enclosure doesn't cover our entire reactor setup, the exhaust or other hazardous fumes may easily be plumbed to the enclosure for safe removal.

4. Conclusions

Here, we applied the anticipate, recognize, evaluate, control, and confirm (ARECC) principles of modern IH/OEHS good practice[27] to (1) anticipate that equipment and systems in nanotechnology laboratory settings can present hazards to workers and researchers, (2) recognize the potential for inhalation exposures to RCF insulation fibers from split-tube furnaces depending on operation and use, (3) evaluate the nature of the potential hazard and exposures and options for exposure mitigation, (4) control inhalation exposures through design and implementation of an adaptable furnace engineering control enclosure, and (5) confirm though quantitative measurements of airborne particle releases that the enclosure design provides the desired protection from risks to workers and researchers.

We found that peak particle and fiber concentrations exceeded time-weighted permissible limits, which indicated that it is possible to surpass these limits depending on use scenarios. We established that uncovered furnace use poses an occupational risk through episodic exposure, which was highly variable from between agitation events. Aerosol particles and fibers were generated through use and their concentrations had a wide range of values. We measured these concentrations under one type of use scenario in one environment. However, other use scenarios and operator practices may result in higher or lower RCF aerosol concentrations. Other types of scenarios include use of multiple furnaces in the same space and use of fans for fast cooling of the insulation, which we reason would affect resultant fiber concentrations. Further, differences in air flow environments, such as ventilation rate, may affect operator exposure in the absence of an engineering control. With this publication we seek to promote environmental health and safety across multiple disciplines by making our economical custom engineering control design accessible to researchers who use furnaces that contain RCFs. The furnace enclosure computer-aided design (CAD) files and technical drawings are available by contacting the corresponding author for ready reproduction of this adaptable engineering control.

Conflicts of interest

The authors have no conflicts of interest to declare.

Acknowledgements

We thank our reviewers for their insightful comments, which strengthened the manuscript, and their recognition of the value of this contribution. This work was supported by the NSF Graduate Research Fellowship Program, Yale University graduate fellowship, MIT's Environment, Health, and Safety Office, and the MIT Central Machine Shop.

References

1 W. Shi, K. Xue, E. R. Meshot and D. L. Plata, The carbon nanotube formation parameter space: data mining and mechanistic understanding for efficient resource use, *Green Chem.*, 2017, **19**(16), 3787–3800, DOI: **10.1039/c7gc01421j**.
2 S. Bhaviripudi, X. Jia, M. S. Dresselhaus and J. Kong, Role of kinetic factors in chemical vapor deposition synthesis of uniform large area graphene using copper catalyst, *Nano Lett.*, 2010, **10**(10), 4128–4133.
3 P. Ahmad, M. U. Khandaker, Z. R. Khan and Y. M. Amin, Synthesis of boron nitride nanotubes via chemical vapour deposition: A comprehensive review, *RSC Adv.*, 2015, **5**(44), 35116–35137.
4 S. Zhang, S. F. Jiang, B. C. Huang, X. C. Shen, W. J. Chen and T. P. Zhou, *et al.*, Sustainable production of value-added

carbon nanomaterials from biomass pyrolysis, *Nat. Sustain.*, 2020, **3**(9), 753–760.
5 Y. M. Manawi, S. A. Ihsanullah, T. Al-Ansari and M. A. Atieh, A review of carbon nanomaterials' synthesis via the chemical vapor deposition (CVD) method, *Materials*, 2018, **11**(5), 822, DOI: **10.3390/ma11050822**.
6 X. Wang, X. Chu, H. Zhao, S. Lu, F. Fang and J. Li, *et al.*, Controllable Growth of Functional Gradient ZnO Material Using Chemical Vapor Deposition, *Integr. Ferroelectr.*, 2014, **151**(1), 1–6.
7 M. Meindlhumer, J. Zalesak, R. Pitonak, J. Todt, B. Sartory and M. Burghammer, *et al.*, Biomimetic hard and tough nanoceramic Ti-Al-N film with self-assembled six-level hierarchy, *Nanoscale*, 2019, **11**(16), 7986–7995.
8 Y. Yuncheng, Z. Tian, L. Jinsong, H. Tingsong and T. Guoan, Chemical Vapor Deposition and Application of Graphene-Like Tungsten Disulfide, *Prog. Chem.*, 2015, **27**(11), 1578–1590.
9 National Institute for Occupational Safety and Health (NIOSH), *Criteria for a Recommended Standard Occupational Exposure to Refractory Ceramic Fibers*, Department of Health and Human Services, Centers for Disease Control Prevention, National Institute for Occupational Safety and Health, DHHS (NIOSH) Publication No. 2006–123, Cincinnati, OH, 2006.
10 L. D. Maxim and M. J. Utell, Review of refractory ceramic fiber (RCF) toxicity, epidemiology and occupational exposure, *Inhalation Toxicol.*, 2018, **30**(2), 49–71, DOI: **10.1080/08958378.2018.1448019**.
11 R. W. Mast, Studies on the Chronic Toxicity (Inhalation) Of Four Types of Refractory Ceramic Fiber in Male Fischer 344 Rats, *Inhalation Toxicol.*, 1995, **7**(4), 425–467, DOI: **10.3109/08958379509015208**.
12 International Agency for Research on Cancer (IARC), *IARC monographs on the evaluation of carcinogenic risks to humans: man-made vitreous fibers (Volume 81)*, World Health Organization, Lyon, 2002, vol. 81.
13 U.S. Environmental Protection Agency (EPA), *Refractory ceramic fibers: Integrated Risk Information System (IRIS) Chemical Assessment Summary*, National Center for Environmental Assessment, 1992.
14 Lindberg Unit Environmental, Safety, and Health Department, *Moldatherm® Insulation Material Safety Data Sheet*, Watertown, WI, 1992.
15 Rex Materials Group, *Safety Data Sheet: Moldatherm, Mixture containing Refractory Ceramic Fibers (RCF)/Alumino- Silicate Wools (ASW)*, SDS No 5036, 2015, pp. 1–11.
16 G. Oberdörster, Determinants of the pathogenicity of man-made vitreous fibers (MMVF), *Int. Arch. Occup. Environ. Health*, 2000, **73**(SUPPL), 60–68.
17 M. J. Utell and L. D. Maxim, Refractory ceramic fibers: Fiber characteristics, potential health effects and clinical observations, *Toxicol. Appl. Pharmacol.*, 2018, **361**, 113–117.
18 H. Greim, M. J. Utell, L. D. Maxim and R. Niebo, Perspectives on refractory ceramic fiber (RCF) carcinogenicity: Comparisons with other fibers, *Inhalation Toxicol.*, 2014, **26**(13), 789–810.
19 R. W. Mast, L. D. Maxim, M. J. Utell and A. M. Walker, Refractory ceramic fiber: Toxicology, epidemiology, and risk analyses - A review, *Inhalation Toxicol.*, 2000, **12**(5), 359–399.
20 T. W. Hesterberg, G. Chase, C. Axten, W. C. Miller, R. P. Musselman and O. Kamstrup, *et al.*, Biopersistence of synthetic vitreous fibers and amosite asbestos in the rat lung following inhalation, *Toxicol. Appl. Pharmacol.*, 1998, **155**(3), 292.
21 E. E. McConnell, R. W. Mast, T. W. Hesterberg, J. Chevalier, P. Kotin and D. M. Bernstein, *et al.*, Chronic Inhalation Toxicity of a Kaolin-Based Refractory Ceramic Fiber in Syrian Golden Hamsters, *Inhal. Toxicol.*, 1995, **7**(4), 503–532, DOI: **10.3109/08958379509015210**.
22 R. W. Mast, T. W. Hesterberg, L. R. Glass, E. E. McConnell, R. Anderson and D. M. Bernstein, Chronic inhalation and biopersistence of refractory ceramic fiber in rats and hamsters, *Environ. Health Perspect.*, 1994, **102**(Suppl 5), 207–209.
23 Testing Consent Order for Refractory Ceramic Fibers, Environmental Protection Agency (EPA), Federal Register/Rules and Regulations, May 14, 1993, vol. 59, no. 93.
24 L. D. Maxim, J. Allshouse, R. E. Fairfax, T. J. Lentz, D. Venturin and T. E. Walters, Workplace Monitoring of Occupational Exposure to Refractory Ceramic Fiber—A 17-Year Retrospective, *Inhalation Toxicol.*, 2008, **20**(3), 289–309, DOI: **10.1080/08958370701866040**.
25 California Division of Occupational Safety and Health (Cal/OSHA) Permissible Exposure Limits (PELs), *Table AC-1 Permissible Exposure Limits for Chemical Contaminants*, Department of Industrial Relations, **https://www.dir.ca.gov/title8/ac1.pdf**.
26 L. D. Maxim, J. N. Allshouse, W. P. Kelly, T. Walters and R. Waugh, A Multiyear Workplace-Monitoring Program for Refractory Ceramic Fibers: Findings and Conclusions, *Regul. Toxicol. Pharmacol.*, 1997, **26**(2), 156–171, DOI: **10.1006/rtph.1997.1153**.
27 AIHA, *AIHA (2022) Competency Framework: Understanding and Applying ARECC to Occupational and Environmental Health and Safety*, American Industrial Hygiene Association, Falls Church, VA, 2022, Available from: **https://www.aiha.org/education/frameworks/competency-framework-understanding-how-arecc-works-within-occupational-exposure-assessment**.
28 TSI Incorporated, *DustTrak DRX Aerosol Monitor Theory of Operation*, 2012, pp. 1–4.
29 X. Wang, G. Chancellor, J. Evenstad, J. E. Farnsworth, A. Hase and G. M. Olson, *et al.*, A novel optical instrument for estimating size segregated aerosol mass concentration in real time, *Aerosol Sci. Technol.*, 2009, **43**(9), 939–950.
30 TSI, *DustTrak DRX Aerosol Monitor Model 8533/8534/8533EP, Operation and Service Manual*, 2019.
31 National Institute for Occupational Safety and Health (NIOSH), *Asbestos by TEM Method 7402, NIOSH Manual of Analytical Methods (NMAM)*, 4th edn, 1994, issue 2.
32 National Institute for Occupational Safety and Health (NIOSH), *Absestos and Other Fibers by PCM – Method 7400,*

NIOSH Manual of Analytical Methods (NMAM), 5th edn, 2019, issue 3.

33 P. N. Breysse, P. S. J. Lees and B. C. Rooney, Comparison of NIOSH Method 7400 A and B Counting Rules for Assessing Synthetic Vitreous Fiber Exposures, *Am. Ind. Hyg. Assoc. J.*, 1999, **60**(4), 526–532, DOI: **10.1080/00028899908984474**.

34 Bureau Veritas North America Inc, *Internal Method: Refractory Ceramic Fiber Analysis Protocol. Quality Assurance Project Plan*, 1991.

35 M. A. Moore, P. M. Boymel, L. D. Maxim and J. Turim, Categorization and nomenclature of vitreous silicate wools, *Regul. Toxicol. Pharmacol.*, 2002, **35**(1), 1–13, DOI: **10.1006/rtph.2001.1509**.

36 Occupational Safety and Health Administration (OSHA), *Permissible Exposure Limits - Annotated Table Z-1 and Table Z-3 Mineral Dusts*, Available from: **https://www.osha.gov/annotated-pels/table-z-1**.

37 Occupational Safety and Health Administration (OSHA), *Asbestos, All Forms*, Available from: **https://www.osha.gov/chemicaldata/231**.

38 *How Much Does a Fume Hood Cost? National Laboratory Sales*, 2021, Available from: **https://www.nationallaboratorysales.com/blog/how-much-does-a-fume-hood-cost/**.